

Article

Estimation of the Deep Geothermal Reservoir Temperature of the Thermal Waters of the Active Continental Margin (Okhotsk Sea Coast, Far East of Asia)

Ivan V. Bragin ¹, Elena V. Zippa ^{1,2,*}, George A. Chelnokov ^{1,3} and Natalia A. Kharitonova ^{1,4}

- ¹ Far East Geological Institute, Far East Branch of Russian Academy of Science, 690022 Vladivostok, Russia; bragin_ivan@mail.ru (I.V.B.); geowater@mail.ru (G.A.C.); tchenat@mail.ru (N.A.K.)
- ² Tomsk Branch of the Trofimuk Institute of Petroleum Geology and Geophysics, Siberian Branch of Russian Academy of Sciences, 634055 Tomsk, Russia
- ³ Geological Institute, Russian Academy of Science, 119017 Moscow, Russia
- ⁴ Geological Faculty, Lomonosov Moscow State University, 119991 Moscow, Russia
- * Correspondence: zev-92@mail.ru

Abstract: Low-enthalpy thermal waters (30–70 °C) with nitrogen as a dominant associated gas are spread within the active continental margin of the Russian Far East (east and north of the Okhotsk Sea Coast) and traditionally are of great importance for recreation and balneology facilities. The thermal waters are chemically classified into three groups: (i) Na–HCO₃(SO₄) type, with low TDS (0.2 g/L) and lowest temperature (<50 °C) and high pH (9.1–9.3), (ii) Na–SO₄ type with TDS (~1 g/L), highest temperature (70 °C) and weak alkaline pH (8.7) and (iii) Ca–Na–Cl type with high TDS (15 g/L), moderate T (59 °C) and neutral pH (7.5). The $\delta^{18}\text{O}$ and δD values suggest that the thermal waters originate from meteoric water, and they are not isotopically fractionated. Silica and cation geothermometers and thermodynamic equilibrium calculations using the GeoT and PHREEQC programs indicate a reservoir temperature for the Na–HCO₃(SO₄) type thermal waters of 103–121 °C and for Na–SO₄ and Ca–Na–Cl types of 136 and 153 °C, respectively. The evaluation of the mixing degree of the thermal water with cold groundwater shows that the equilibration temperature ranges between 148 and 153 °C. Estimated circulation depths for thermal manifestations range from 2.7 to 4.3 km and may be as great as 6 km.

Keywords: thermal waters; temperature estimation; geothermometers; mixing diagram



Citation: Bragin, I.V.; Zippa, E.V.; Chelnokov, G.A.; Kharitonova, N.A. Estimation of the Deep Geothermal Reservoir Temperature of the Thermal Waters of the Active Continental Margin (Okhotsk Sea Coast, Far East of Asia). *Water* **2021**, *13*, 1140. <https://doi.org/10.3390/w13091140>

Academic Editor: Zhonghe Pang

Received: 17 March 2021

Accepted: 20 April 2021

Published: 21 April 2021

Publisher's Note: MDPI stays neutral with regard to jurisdictional claims in published maps and institutional affiliations.



Copyright: © 2021 by the authors. Licensee MDPI, Basel, Switzerland. This article is an open access article distributed under the terms and conditions of the Creative Commons Attribution (CC BY) license (<https://creativecommons.org/licenses/by/4.0/>).

1. Introduction

The low-enthalpy N₂-dominated thermal waters of the active continental margin of the Russian Far East are widespread along the coasts of the Sea of Japan and the Sea of Okhotsk [1,2]. Some thermal waters, represented as natural springs, and others have been discovered as a result of drilling in 1930s–1960s [1]. Most of these waters are actively used as spa centers by the populace for therapeutic and balneological purposes, whereas others are used by locals as spa for self-treatment. During the last two decades, the geochemistry of thermal group of springs located on the south of the area has been studied [1–9]. Although the thermal waters of the Magadan region are formed in the permafrost zone, annual fluctuations in the flow rate and/or the chemical composition of the waters have been observed scarcely [5,6]. Geochemistry of northern thermal areas (Talaya and Tavatum) have not been applied in elucidating the origin, heat source, geothermal reservoir temperature, geothermometric methods or mixing ratio of thermal and cold water, until the present day.

Geothermal systems in non-volcanic continental margins are mostly of crustal origin and are associated with the decay of radioactive elements (e.g., ²³⁸U, ²³²Th, ⁴⁰K), unlikely to have magmatic heat sources [10,11]. Another heat source is that developed along with interfaces between lithospheric sectors, where friction and viscous shearing forces along boundaries are converted into heat [12].

Silica and cation geothermometers, the Na–K–Mg ternary diagram, the silica–enthalpy model and the thermodynamic equilibrium method have widely been used as tools in estimating the reservoir temperatures of geothermal systems, based on chemical analyses of the thermal waters [10,13]. After a cross-validation of the results from each method in this research, suitable methods were adapted to estimate the reservoir temperature of the thermal waters, because of the different range of their applicable temperature and given chemical data condition.

The aims of the study were to determine the chemical and isotopical composition of the thermal manifestations of Okhotsk Sea Coast, in order to estimate the geothermal reservoir temperature using geothermometers, the thermodynamic equilibrium method and the silica–enthalpy model, which have their intrinsic applicable temperature range.

2. Site Description

The five main thermal manifestations (Annenskie, Tumnin, Ul'skiy, Talaya and Tavatum) are known and located along of continental Okhotsk Sea Coast. According to tectonic schemes of region Talaya and Tavatum thermal area belongs to the Okhotsk–Chukotka volcanic belt (the Okhotsk and North American Plates consequently), whereas others occur within the east Sikhote–Alin volcanic belt (the Amur Plate) (Figure 1). Consider these thermal areas based on these conditions.

The 3200 km long Okhotsk–Chukotka volcanic belt of NE Eurasia appears to be the largest volcanic province spatially related to active continental margins [14]. It constitutes a significant part of the Mesozoic magmatic arc system of the Circum-Pacific [15] and comprises over 1 million km³ of volcanic rocks [14]. Thermal manifestations have a recharge zone exceeding the discharge area by 500–600 m. All thermal waters come to the surface in tectonically weakened zones of river beds or streams. The climate is temperate, continental with a distinct influence of the sea. The greatest amount of precipitation occurs in the summer. Water supply is stable and is carried out mainly by groundwater from deep horizons. Heat flow variations in the Okhotsk–Chukotka volcanic belt consist of 65–84 mW/m² [16].

The Tavatum thermal area is located in the North-Evenskiy district of the region, 2 km from the coast of the Shelikhov bay, in the floodplain of the Khoksichan Creek, the left feeder of the Tavatum River (about 60 m.a.s.l). Within the thermal zone, two artesian wells (125 and 150 m depth) and several natural springs with a total discharge rate of about 6 L/s have occurred [6]. The thermal area is located at the junction of two large tectonic structures of the Verkhoyansk–Kolymskiy fold area: the Gizhiginskaya fold zone and the Sugoiskiy marginal trough superimposed on the structures of the Okhotsk–Chukotka volcanogenic belt. Faults are widely distributed within the territory. The majority of the faults are genetically associated with a tectonically weak zone, feathering the Doktomychanskiy deep fault. Some intrusive formations and the thermal waters are spatially confined to it. Thermal water is confined to the Upper Cretaceous volcanogenic rocks, broken by intrusive formations and largely overlaid by loose Quaternary formations. Dacites, quartz alkaline diorites, diorite porphyries, rhyolites and andesites represent the Late Cretaceous intrusive formations (Figure 2) [17].

The Talaya thermal area is located in the Khasynskiy district of the Magadanskiy region, 270 km to the north from the city of Magadan, on the right bank of the right tributary of the Talaya River, Krivoy Creek (about 670 m.a.s.l). The Talaya resort and spa center uses the thermal water for patients' treatment. Nowadays, thermal water is pumped year-round from one deep well (depth 162 m) with a median debit of about 14 L/s. Thermal water originates in the Upper Triassic–Lower Jurassic sediments (sandstones, siltstones and silty-clay shales), broken through by a series of Upper Cretaceous effusive rocks of the Ol'skaya suite, represented by rhyolites and their tuffs, abraded by erosion processes. Approximately 3 km east of the thermal deposit, the area is cut through by Early Cretaceous granodiorites (Figure 2) [17].

The east Sikhote–Alin volcanic belt (~1500 km long) is commonly regarded as a tectonomagmatic structure formed in the Late Cretaceous in a subduction environment, which was followed by the destruction of the oceanic slab and active asthenospheric diapirism in the Cenozoic [18]. The Sikhote–Alin folded area is mostly represented by mountains (up to 600 m) and hills distributed along the Sea of Japan coast. Heat flow variations in the Sikhote–Alin volcanic belt consist of 39–56 mW/m² [16].

The Ul'sky thermal spring ($T = 26\text{--}32\text{ }^{\circ}\text{C}$) is located on the east of the Khabarovsk region, in the north end of Sikhote–Alin ridge, 25 km from the Sea of Okhotsk shore (about 320 m.a.s.l.). The thermal water of low mineralization ($\text{TDS} = 0.1\text{--}0.2\text{ g/L}$) and water discharge (0.15 L/s) is associated with the fractured zones of the Paleogene intrusion (Figure 2) [3,17]. Thermal area is associated with the Bekchiul granitic massif of Paleocene age (Figure 2). The location of the massif is determined by the deep-seated fault of the north-eastern course. The granitoid are ascribed to the Verkhneudominskii gabbro–granite complex according to the geological map and marked out as the specific Bekchiul diorite–granite plutonic complex given the map [7] (Figure 2). The rocks are represented by biotite–hornblende and pyroxene–hornblende granodiorites and granosyenites characterized by gradual interconversions and wide structural variations. The rocks in the deep cuttings are characterized by medium- and coarse-grained structures alternating towards the cover with fine-grained and porphyry forms [7]. The cover flexures within the bounds of the massif are constituted by Upper Jurassic and Lower Cretaceous sedimentary formations along with Upper Cretaceous vulcanites. The parameters of the oxygen and hydrogen isotopes [3] point to the infiltration genesis of the waters and are in good agreement with the latitudinal regularity of the region according to the available data [19].

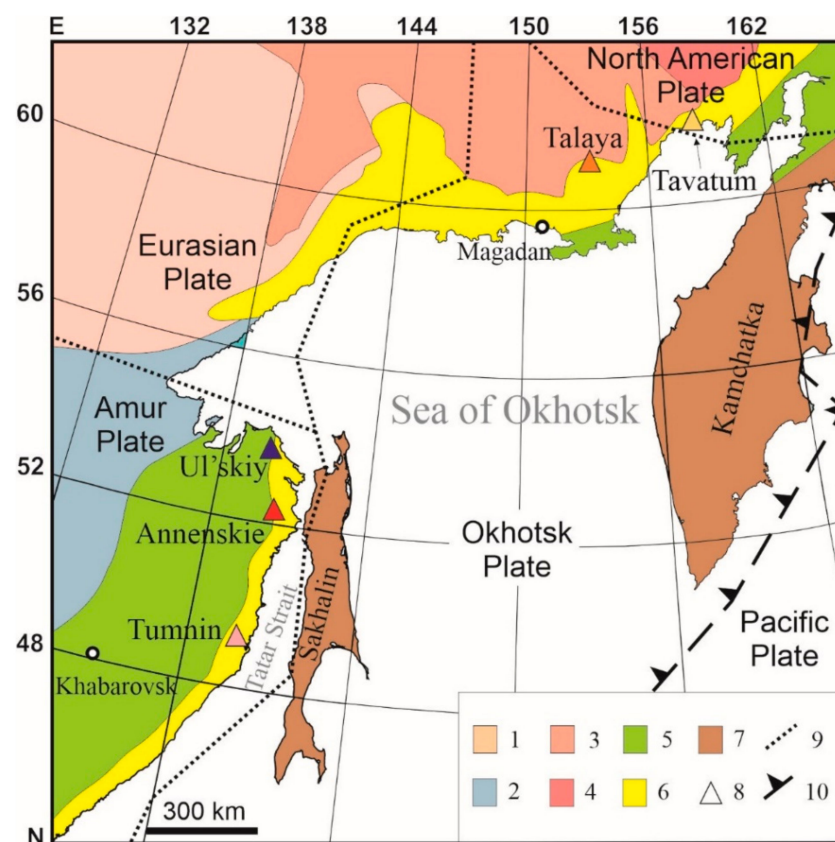


Figure 1. Tectonic sketch map of the studied area with the sampling points. Modified after [16,20]. 1—Siberian Plate, 2—Central Asian Orogenic Belt, 3—Verkhoyansk–Kolyma fold belt, 4—betwixt mountains, 5—Late Mesozoic orogeny, 6—Okhotsk–Chukotka volcanic belt, 7—Cenozoic orogeny, 8—thermal area, 9—Tectonic Plate borders, 10—subduction zone.

The Annenskie thermal water deposit is located in the Ul'chskiy district of the region at the lower reaches of the Amur River, on its right bank, 120 km upstream from the town of Nikolaevsk-On-Amur (about 60 m.a.s.l). The spa resort “Annenskie Vody” uses water from the well of this deposit, serving more than 10,000 people a year [1] (Figure 1). Thermal water occurs in the contact zone between volcanoclastic sedimentary rocks of the Upper Cretaceous of Bolbinskaya and Tatarkinskaya suites. The rocks of the Bolbinskaya suite that host thermal waters are represented by pyroxene–plagioclase porphyrites, tuffs and lava breccias. They are unevenly overlain by tuffs, tuff sandstones and tuffaceous siltstones of the Tatarkinskaya Formation. The main minerals are everywhere replaced by carbonates, chlorite and epidote. The rocks are covered with eluvial–diluvial sediments (thickness up to 5–8 m) consisting of clay, poorly sorted sand and gravel. Hydrogeological settings are determined by tectonic factors in the zone of SE fault with strongly fractured and hydrothermally altered host rocks (Figure 2) [5]. Nowadays, thermal water is pumped from two deep wells (average depth 220 m) with the median debit of about 7 L/s.

The Tumnin Spa is the most southern thermal area located in the Vanino district of the Khabarovsk region and 40 km away from the Tatar strait (about 300 m.a.s.l). The geological structure that is defined by the thermal water was first developed as a commercial hot spa in 1956 from a shallow well in the contact zone of Paleocene granitoids (granodiorites, syenite-diorites and granites) and effusive rocks of Miocene (andesite basalts and tuffs) [5]. Thermal water occurs within the pre-domical zone of the Aichi Mountain and complex tectonic unit formed by the intersection of main arc-pre-domical fault (dropping) with radial (shift) and subhorizontal thrust (Figure 2) [5]. In the zones of influence of thermal waters, processes of secondary mineral formation are intensively developed—kaolinization of feldspars, zeolitization, ferruginization—and in deeper zones exposed by wells—albitization, carbonatization, chloritization, zeolitization. Nowadays, thermal water comes from two deep wells (average depth 245 m) with the median debit of about 12 L/s.

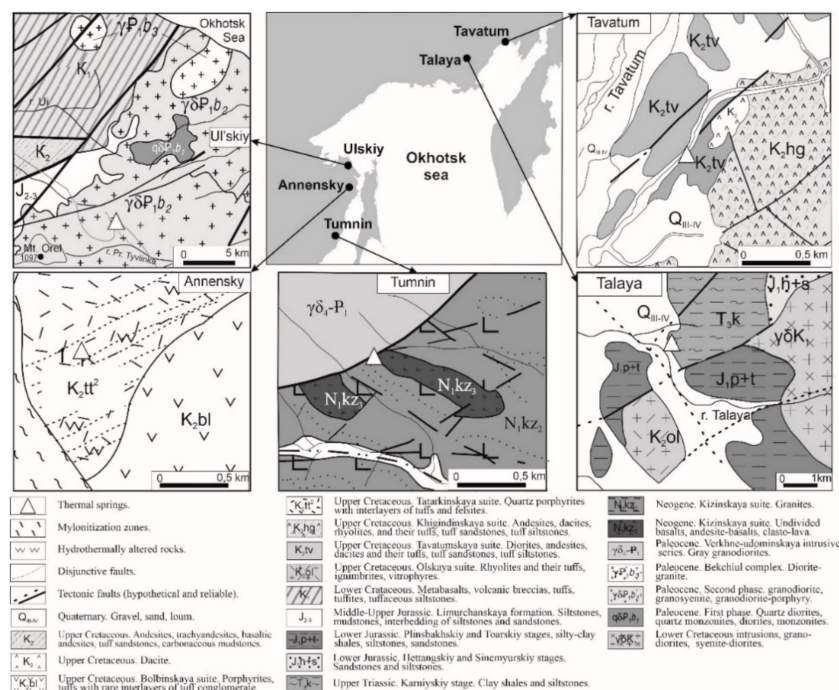


Figure 2. The geological conditions of the studied thermal waters.

3. Materials and Methods

The research is based on the results of hydrochemical sampling held in 2018–2020 for thermal waters of Okhotsk Sea Coast. Five samples of thermal waters and groundwaters were collected during the field works. The thermal waters of Sikhote–Alin region were sam-

pled in September–October, the thermal waters of Okhotskiy region in October–November. These seasons are most comfortable for the field works, and thermal deposits and springs are easy to reach. The water temperature and pH values were measured in situ using an AMTAST AMT03 (Amtast USA Inc., Lakeland, FL, USA) device. The chemical composition analysis was carried out with the liquid ion chromatography method (HPLC-10 Avp, SHIMADZU). Concentrations of Si were determined by the mass spectrometry method (ICP-AES, Agilent iCAP 7600 Duo). The analyses were carried out in the Analytical Center of Far East Geological Institute of the Far Eastern Branch of the Russian Academy of Sciences (AC FEGI FEB RAS) (Vladivostok, Russia). Standard deviations did not exceed 3%. Isotopic analysis of oxygen and hydrogen in water ($\delta^{18}\text{O}$ and δD) was performed on TC/EA high-temperature pyrolyzer (ThermoQuest, Bremen, Germany) connected to a MAT 253 isotope mass spectrometer (ThermoQuest, Bremen, Germany) via a ConFlo-IV interface (ThermoQuest, Bremen, Germany). The results of analyses of δD and $\delta^{18}\text{O}$ are given relative to the international standard VSMOW (Vienna Standard Mean Ocean Water). The reproducibility of the results in the analysis of this series of samples was controlled by repeated measurements of the laboratory standard. The reproducibility of the results averaged ± 0.1 and $\pm 0.7\text{‰}$ for $\delta^{18}\text{O}$ and δD , respectively. Concentrations of SiO_2 were calculated using multiplication factor 2.14 reflecting differences in molar weight of Si and SiO_2 .

Solute geothermometers have been used for decades to infer the temperature of deep geothermal reservoirs from analyses of fluid samples collected at ground surface from springs and exploration wells [21–28]. These “classical” geothermometers and several of their modifications have been successfully applied to many geothermal waters and have become important and essential geothermal exploration tools. These geothermometers connect the depth temperature with the concentration or concentration ratios of the following elements: Si, Na/Li, Na/K, Na–K–Ca. Some works [21,25] suggest the calculation formulas for the estimation of the reservoir temperature based on the SiO_2 solubility depending on the temperature. To estimate this temperature, Si geothermometers were used taking into account silica species (quartz, cristobalite, chalcedony) and temperature ranges. In this work, the Si geothermometer for adiabatic (1), conductive solution cooling (2) and chalcedony geothermometers were used for the calculation of the depth temperature [21]:

$$T, \text{ }^\circ\text{C} = 1522 / (5.75 - \log(\text{SiO}_2)) - 273.15, \quad (1)$$

$$T, \text{ }^\circ\text{C} = 1309 / (5.19 - \log(\text{SiO}_2)) - 273.15, \quad (2)$$

$$T, \text{ }^\circ\text{C} = 1032 / (4.69 - \log(\text{SiO}_2)) - 273.15, \quad (3)$$

where T ($^\circ\text{C}$) is the equilibration temperature at depth, and SiO_2 – is the silica concentration, mg/L. Additionally, the silica geothermometer (2) has shown promise in estimating circulation depths for “cold” springs having temperatures in the range of 3–25 $^\circ\text{C}$ [29].

The Na–K geothermometer is less affected by the boiling and cooling processes because the concentration ratio is used instead of absolute value, unlike the Si geothermometer. Therefore, the reservoirs’ temperature of the studied thermal waters was estimated also using Na–K geothermometer and Na–K–Ca geothermometer according to Equations (5)–(7) [22–24]:

$$T, \text{ }^\circ\text{C} = [1217 / (1.483 + \log(\text{Na}/\text{K}))] - 273.15 \quad (4)$$

$$T, \text{ }^\circ\text{C} = [1178 / (1.470 + \log(\text{Na}/\text{K}))] - 273.15 \quad (5)$$

$$T, \text{ }^\circ\text{C} = [1647 / (\log(\text{Na}/\text{K}) + \beta(\log(\text{Ca}/\text{Na}) + 2.24))] - 273.15 \quad (6)$$

if $(\log(\text{Ca}/\text{Na}) + 2.06) < 0$, then use $\beta = 1/3$; if $(\log(\text{Ca}/\text{Na}) + 2.06) > 0$, then use $\beta = 4/3$; if obtained temperature $T > 100$ $^\circ\text{C}$, then recalculate using (5), where $\beta = 1/3$ [24].

Na/Li geothermometer was used for the estimation of the reservoirs' temperature of thermal waters with a high concentration of chlorine⁻ (6) [18]:

$$T, ^\circ\text{C} = [1195 / (0.130 + (\log(m\text{Na} / m\text{Li})) - 273.15 \quad (7)$$

The degree of the thermal waters mixing with cold groundwater was estimated using the Si-enthalpy mixing diagram also allowing determination of the temperature at the circulation depth with more accuracy [15,16]. Concentration of SiO₂ for cold groundwater was taken from regional paper [2].

We used the GeoT software based on the multicomponent chemical geothermometry method presented by Reed and Spycher [30] and further developed by Pang and Reed [31] and Palandri and Reed [32] to make a cross-check validation of the "classical" geothermometers. The method consists of using full chemical analyses of water samples to compute the saturation indices ($\log(Q/K)$) of reservoir minerals over a range of temperatures (e.g., 20 to 200 °C). The saturation indices were graphed as a function of temperature, and the clustering (RMED) of $\log(Q/K)$ curves near-zero at any specific temperature (for a group of certain reservoir minerals) is inferred to yield the reservoir temperature. Unknown concentrations of one or more specific elements in the deep fluid can be optionally computed by assuming that the concentration of each element is constrained by the thermodynamic equilibrium between that element and a respective mineral, resulting in a so-called "Fix-Al" method for aluminum [31].

4. Results

4.1. Chemical and Isotopic Composition

The chemical composition of studied waters is listed in Table 1 and on the Piper diagram (Figure 3), which demonstrates the proportions between the water components. The waters of the Sikhote–Alin volcanogenic belt (Tumnin, Annenskie, Ul'skiy) are alkaline and ultra-fresh, while the thermal waters of the Okhotsk–Chukotka volcanic belts (Talaya and Tavatum) are brackish or salt and weakly alkaline and neutral.

Table 1. Chemical composition of the Okhotsk Sea Coast thermal waters.

Name	T	TDS	pH	HCO ₃ ⁻ + CO ₃ ²⁻	Cl ⁻	SO ₄ ²⁻	Na ⁺	K ⁺	Ca ²⁺	Mg ²⁺	SiO ₂	δ ¹⁸ O	δD
	°C	g/L		mg/L					%o, SMOW				
Tumnin	44	0.2	9.3	78	2	10	34	0.6	0.7	<0.1	73	−16	−117
Annenskie	49	0.2	9.2	112	5	34	59	1.5	2.0	<0.1	88	−18.8	−136
Ul'skiy	31	0.2	9.1	58	5	18	35	0.7	1.6	<0.1	52	−15.5	−113.4
Talaya	70	1.0	8.7	84	57	282	200	13	11	0.20	98	−23.4	−177.9
Tavatum	59	15	7.5	21	11087	131	3516	136	2711	<0.1	76	−16.3	−124.1

All studied thermal waters within the Sikhote–Alin volcanogenic belt have low TDS: 257, 160 and 170 mg/L for Annenskie, Tumnin and Ul'skiy thermal waters, respectively. The pH values for Tumnin thermal water is 9.3, pH of Annenskie thermal spring—9.2, for Ul'skiy—9.1. The temperature at the surface of Annenskie, Tumnin and Ul'skiy thermal waters are 49, 44 and 31 °C, respectively (Table 1). The chemical composition of the thermal waters is characterized by the dominance of HCO₃⁻ among anions and Na⁺ among cations. Concentrations of HCO₃⁻ in Annenskie, Tumnin and Ul'skiy thermal springs are, respectively, 112, 78 and 58 mg/L, Na⁺—59, 34 and 35 mg/L. As for the rest of the anions, the SO₄²⁻ content is lower than HCO₃⁻ in the considering waters and range between 10 and 34 mg/L; Cl⁻ concentrations do not exceed 5 mg/L. Besides, the thermal waters contain high concentrations of SiO₂: in Annenskie thermal deposit is 88 mg/L, Tumnin—73 mg/L, Ul'skiy—52 mg/L (Table 1). According to the chemical composition, the considering waters belong to HCO₃–Na (Tumnin) and HCO₃–SO₄–Na (Annenskie and Ul'skiy) types (Figure 3).

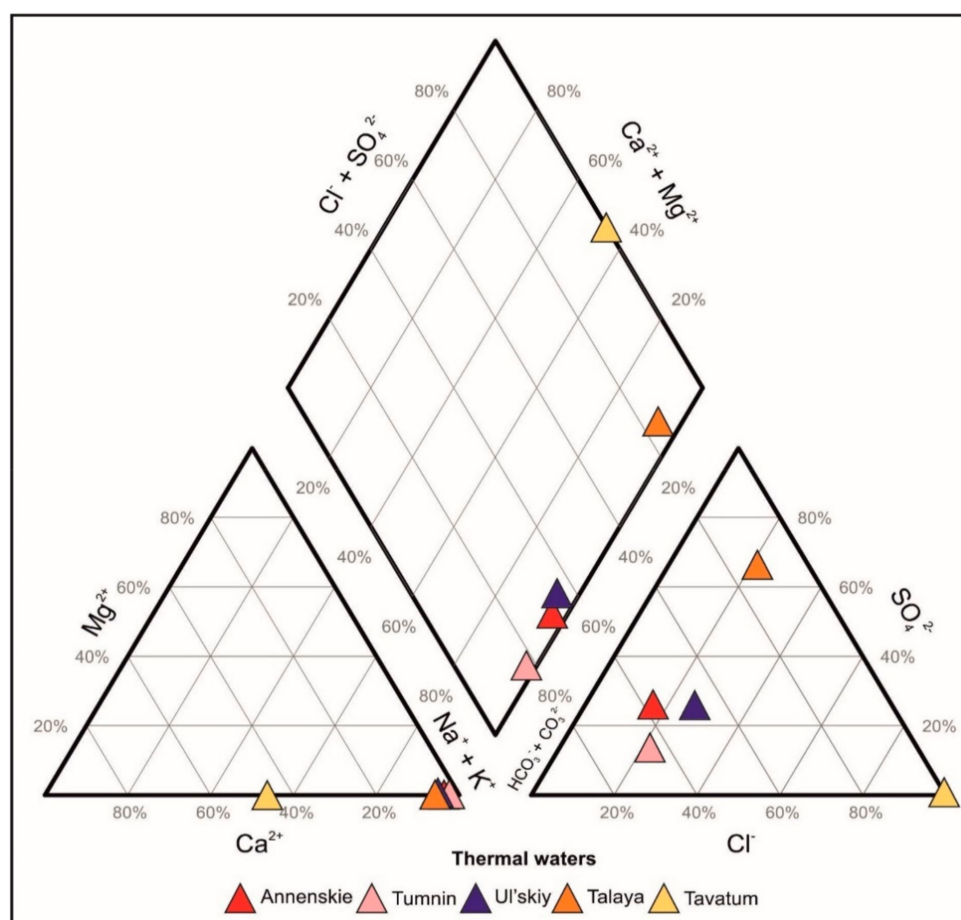


Figure 3. The Piper diagram for the Okhotsk Sea Coast thermal waters.

The thermal waters of the Okhotsk–Chukotka volcanic belt belong to $\text{SO}_4\text{--Na}$ and Cl--Ca--Na chemical types (Figure 3). The TDS value for Talaya thermal water is 1 g/L, and the pH value is 8.7. This thermal water has the highest discharge temperature (70 °C). The Talaya thermal waters composition is characterized by the significant dominance of SO_4^{2-} among anions where the concentration is 282 mg/L. Lower concentrations are obtained for HCO_3^- (84 mg/L) and Cl^- (57 mg/L). Na^+ dominates among cations and reaches 200 mg/L. Concentrations of K^+ , Ca^{2+} , Mg^{2+} for Talaya thermal water are, respectively, 13, 11 and 0.2 mg/L. This water contains SiO_2 of 98 mg/L (Table 1). According to the chemical composition, the Talaya thermal waters belong to $\text{SO}_4\text{--Na}$ (Figure 3). The Tavatum thermal spring is the saltiest in the group and alkaline comparing with thermal waters considering above. The TDS value for the Tavatum waters is 15 g/L, and pH is 7.5. The spring temperature at the surface is 59 °C. The Tavatum thermal water boasts an extremely high concentration of Cl^- among anions reaching 11 g/L. The water contains HCO_3^- and SO_4^{2-} in smaller amounts: 21 and 131 mg/L, respectively. Among cations, Na^+ and Ca^{2+} are dominant with concentrations 3.5 and 2.7 g/L, respectively. The concentration of K^+ reached 136 mg/L, the Mg^{2+} content is significantly low and does not exceed 0.1 mg/L. The concentration of SiO_2 is 76 mg/L. According to the chemical composition, the Tavatum thermal spring belongs to the Cl--Ca--Na chemical type (Figure 3). The calcium enrichment of waters and low concentrations of sulfate ion and magnesium are characteristic of metamorphosed sedimentogenic marine waters when magnesium is bound by clay minerals and carbonates, and the sulfate is consumed in the process of sulfate reduction. Similar patterns were previously observed for the thermal waters of Chukotka [9], which may probably be a regional feature.

The isotopic (δD , $\delta^{18}\text{O}$) data for all studied waters are presented in Table 1. First time obtained data on Talaya and Tavatum thermal waters with data on Sikhote–Alin

springs [2,5] demonstrate that isotopic values are similar to the meteoric water values with a significant latitude effect (more depleted water being recharged at higher altitudes and migrating deeper into the heat source). During the hydration of silicate minerals. The oxygen shift due to oxygen isotopic exchange in water–rock interactions, as observed in high-temperature thermal waters [33], is not observed in the studied thermal waters.

4.2. Estimation of the Reservoir Temperature

The calculation results of the thermal waters' temperature at the circulation depth are presented in Table 2. The temperatures calculated using the Si geothermometer for adiabatic and conductive cooling [21] are slightly different. In the case of using the Si geothermometer for conductive cooling, the calculated temperatures range from 103 to 136 °C.

Table 2. The results of the reservoir temperature calculations, °C.

Thermal Water	T _{meas.}	(1)	(2)	(3)	(4)	(5)	(6)	(7)
Tumnin	44	119	121	92	200	100	121	107
Annenskie	49	127	130	103	225	121	141	172
Ul'skiy	31	104	103	74	202	108	129	212
Talaya	70	132	136	109	306	181	198	366
Tavatun	59	120	123	94	268	147	166	153
Minimum	31	104	103	74	200	100	121	107
Maximum	70	132	136	109	306	181	198	366

Number in the first line indicates the formula for calculations (see Materials and Methods). T_{meas.}—measured temperature of thermal water.

In the case of the Si geothermometer for adiabatic cooling, the reservoir temperatures range between 104 and 132 °C. Temperatures estimated with Na–K–Ca [24] and Na/K geothermometers [22,23] range from 200 to 306 °C and from 100 to 198 °C, respectively. The significant range of the reservoir temperature was obtained using Na/Li geothermometers [28] and is 21–366 °C.

The Giggenbach's triangular diagram (Figure 4) [23] is used to establish the correctness of the use of Na–K geothermometers when assessing the temperatures of reservoirs. For clarity, points are plotted, reflecting the ratio of the concentrations of cations in thermal waters (wells) and natural thermal springs. It can be seen that some waters are located in the area of the so-called "immature waters", according to [23], in other words, waters that have not reached equilibrium with the host rocks. For such waters, temperature calculations will be incorrect. The values of thermal waters are located at the boundary of waters in equilibrium with rocks, in the temperature ranges from 60 to 150 °C (Figure 4).

The obtained temperatures require additional explanation and show that the certain geothermometer taking into account formation conditions, composition peculiarities and usage limitations should be applied for the certain thermal waters. Sources of uncertainty in geothermometry include (i) mixing of cool, shallow-circulating groundwater with warm, deep-circulating groundwater, (ii) disequilibrium between the groundwater and minerals may not be achieved, and (iii) the geothermal gradient may be cooler/warmer than published data indicate [34]. With regards to the first source of uncertainty, if upwelling thermal groundwater that may have circulated to a great depth mixes with younger, cooler groundwater near the spring emergence, then this would ultimately lead to dilution of the silica composition [24,29,35]. Dilution, in turn, leads to the underestimation of the equilibration temperature and circulation depth.

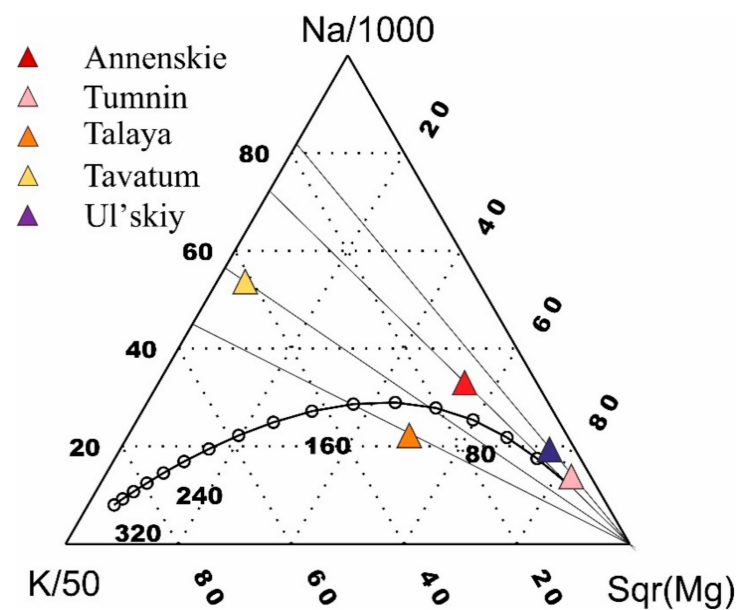


Figure 4. Content of K, Na and Mg in thermal waters of the Okhotsk Sea coast.

To estimate the degree of the thermal waters mixing with cold groundwater and surface water and to evaluate with more accuracy the reservoir temperature, the Si-enthalpy mixing model can be used (Figure 5) [25,26,36–44].

The line through the point of the coldest mixing component (groundwater) and the point of mixed hot water (the considering springs) crossing the quartz solubility line gives the intersection points with values of silica in milligram per liter and the enthalpy for the thermal waters in joule per gram, and the resulting line is called the mixing line [25,26]. The boiling process should also be taken into account using the Si-enthalpy mixing model. If there is no steam separation before mixing, the intersection point of the mixing line and the quartz solubility line provides the enthalpy values and consequently temperature values of the reservoir. In case of steam separation occurring before mixing, the intersection point of the mixing line and the line corresponding to the boiling temperature ($T = 100\text{ }^{\circ}\text{C}$, $H = 419\text{ J/g}$) is connected with maximum steam loose line parallel to the enthalpy axes. The obtained intersection provides values of enthalpy and temperature [25,26]. The correlation between enthalpy and temperature values are determined according to reference data [29,45]. Figure 5 shows that thermal waters of the Okhotsk Sea Coast were mixed with cold groundwater during the rising to the surface. If steam separation occurs before mixing, the intersection points A, C, E, G and I provide the reservoir temperature of the considering thermal waters from $145\text{--}162\text{ }^{\circ}\text{C}$. However, if there is no steam separation before mixing, the intersection point of the mixing line and quartz solubility points B, D, F, H and I provide the reservoir temperature ranging between $200\text{--}253\text{ }^{\circ}\text{C}$ (Figure 5, Table 3).

We added two points to this figure to compare the obtained results with reference data for geothermal systems of the active volcanic zone of Kamchatka [46,47]. The reservoir temperature of Paratunka thermal water in case of steam separation before mixing is $130\text{ }^{\circ}\text{C}$ ($H = 546\text{ J/g}$), in case of stem separation occurring after mixing $152\text{ }^{\circ}\text{C}$ (640 J/g). According to Figure 5, the mixing line for the Vilyuchinsk thermal water does not cross the line of quartz solubility that signifies the considering thermal water was not mixed with cold groundwater. In this case, the reservoir temperature can be defined as the cross point of quartz solubility line with the line connecting steam point with thermal spring (Figure 5). The point M projection to enthalpy axis shows values 671 J/g that provides the temperature of $159\text{ }^{\circ}\text{C}$.

Table 3. Results of the reservoir temperature estimation using the Si-enthalpy mixing model.

Thermal Water	Steam Separation before/after Mixing	The Point in Figure 4	H, J/g	T, °C
Annenskie	before	A	684	162
	after	B	1100	253
Tumnin	before	C	671	159
	after	D	1047	242
Ul'skiy	before	E	675	160
	after	F	1090	251
Talaya	before	G	619	147
	after	H	861	202
Tavatun	before	I	610	145
	after	J	861	202
Paratunka [46]	before	K	546	130
	after	L	640	152
Vilyuchinsk [47]	no mixing	M	671	159

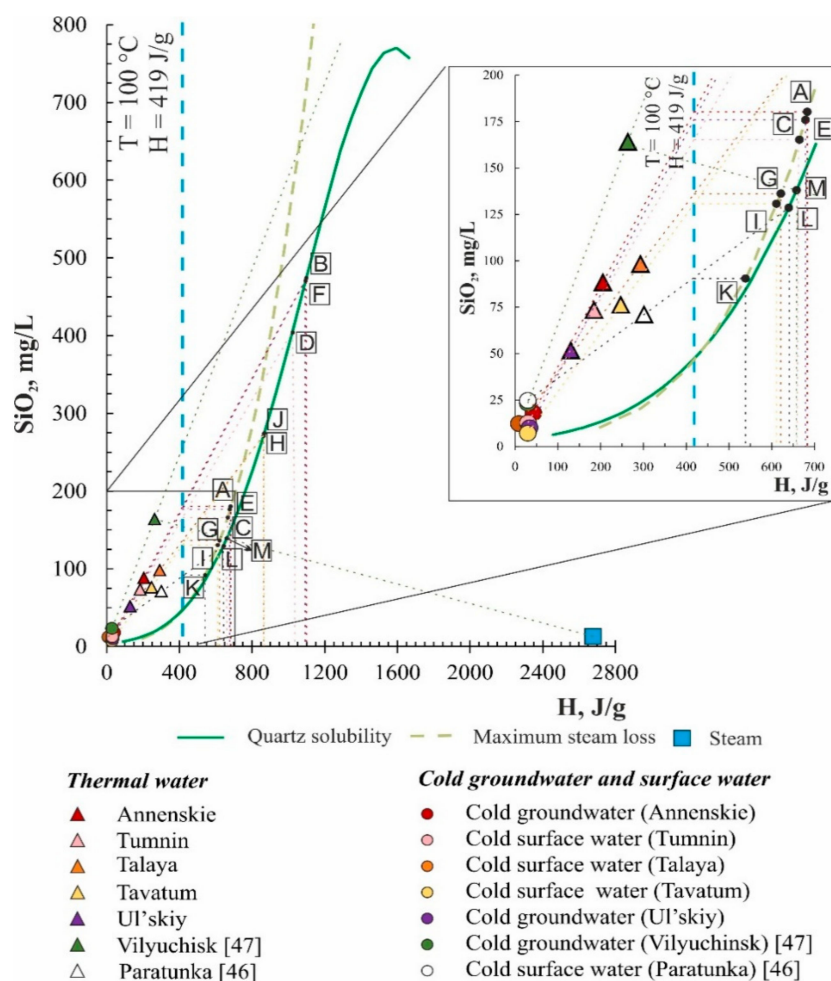


Figure 5. Silica-enthalpy mixing model for Okhotsk Sea Coast thermal water.

The results of computing the saturation indexes for studied waters for the interval of temperatures of 20–200 °C are presented in Figure 6. A mineral assemblage is adopted based on the literature [1,3,5,7], which shows that the geothermal reservoir of the Tumnin, Ulsky and Annenskie thermal waters relate to granite intrusions, while for the Talaya ther-

mal area, it is clay shales and siltstones. The determination of geothermal reservoir rocks of the Tavatum is more complicated, because it is represented both by effusive volcanic (andesites) and intrusive igneous rocks of intermediate composition (diorites) and sedimentary rocks (siltstones) as well. According to [1,3], the Tumnin, Ulsky and Annenskie geothermal reservoirs contain quartz, calcite, actinolite, sanidine, albite, microcline, dolomite, chlorite, heulandite, kaolinite and microcline, calcite, quartz, albite, microcline, laumontite appear in the Talaya and Tavatum geothermal reservoirs. Control of the aluminum concentrations for the Fix-Al model is held by albite.

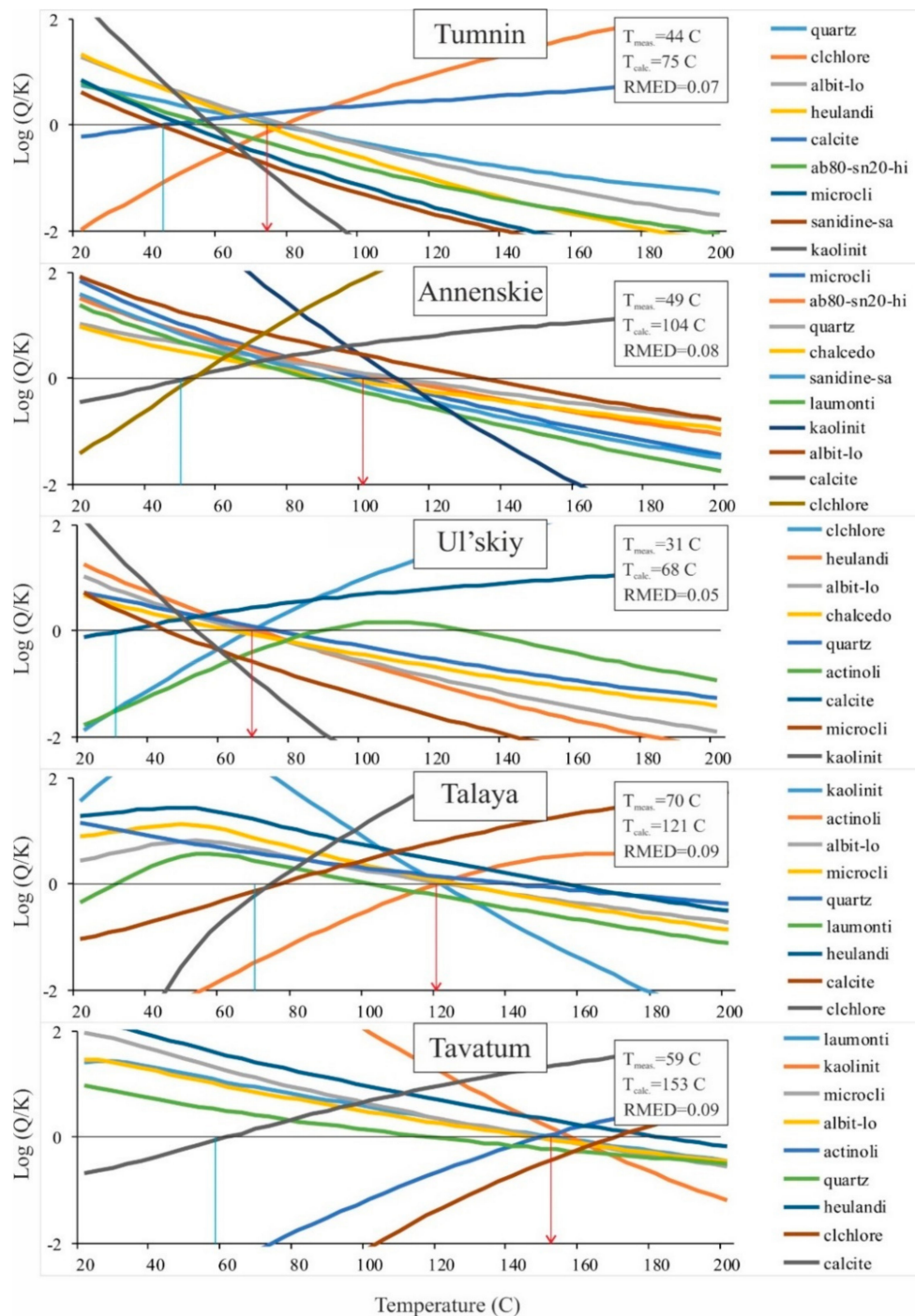


Figure 6. Computed saturation indices, $\log(Q/K)$, as a function of temperature for studied thermal waters. RMED—statistical analyses of saturation indices median of absolute $\log(Q/K)$ values. The reservoir temperature is inferred from the temperature at which RMED is minimum.

5. Discussion

The obtained results of the reservoir temperature estimation show the variety of ranges that require additional explanation. Si geothermometers are more applicable for reservoir conditions > 150 °C. Below this temperature, the chalcedony rather than quartz control the dissolved Si content. The Si geothermometer with adiabatic cooling (maximum steam loss) (1) compensates for the loss of steam from boiling solutions and the resultant increase in the concentration of silica and is best used for wells and vigorously boiling springs. The temperatures of the considering thermal waters at the surface are below boiling one (100 °C); therefore, this geothermometer can be less applicable for the studied waters. In this case, it is better to use the Si geothermometer with conductive cooling. If the quartz geothermometer, and other geothermometers, indicates the temperature of 120–180 °C, it is possible that chalcedony may control silica solubility. Under these circumstances, it is better to use the chalcedony (3) geothermometer [21]. If the chalcedony geothermometer gives temperatures of 100–120 °C, it may represent the true deep temperature. However, if the calculated temperature is below 100 °C, the amorphous silica may control the solubility. At lower temperatures in systems with silicic host rocks, the abundance of volcanic glass may enable saturation of a fluid concerning amorphous silica. In our case, the most reliable results were obtained for Annenskie and Talaya consequently using quartz and chalcedony geothermometer, resulting in 103 and 109 °C, respectively. The results for Tumnin, Ul'skiy and Tavatum are compromised by mixing with cold groundwater leading to disequilibrium of thermal water with main silica minerals.

The Na/K geothermometers is used for waters from high-temperature reservoirs (180 °C), with near-neutral pH, and is less affected by dilution or steam loss, unlike Si geothermometers. Furthermore, according to Table 2, the calculated temperatures do not exceed 180 °C, and pH 7.5 corresponded only for Tavatum spring. Consequently, the Na/K geothermometer maybe not be applied to the studied waters. The Na–K–Ca geothermometer cannot be used for calculating temperatures of the reservoir, since the results are overestimated. Moreover, Na–K–Ca geothermometer is more applicable for waters enriched with Ca^{2+} [24], the concentration of Ca^{2+} in the studied waters does not exceed 2 mg/L, except Talaya and Tavatum thermal waters, but the temperatures are still overestimated. Cation geothermometers are less affected by dilution or steam loss that it is based on a ratio. This is if the diluting waters are low in Na, K and Ca. Note that seawater is not a diluent but the end member fluid of distinct composition. The geothermometer applies to 350 °C, as the re-equilibration is slower than that of the silica–quartz geothermometer. Therefore, the Na–K geothermometer may give indications regarding the deeper part of the system in comparison to the Si geothermometer, depending on the system's hydrology. A slowly rising fluid can, however, re-equilibrate at shallower levels and cooler temperatures. The most suitable geothermometer for high-mineralized thermal water containing more than 0.3 mol/kg of Cl^- , particularly for Tavatum spring, is a Na/Li geothermometer. Therefore, the Tavatum thermal water has 153 °C.

The scatter in the temperature estimates is caused by the complex hydrogeological conditions of the deposits, when in near-surface conditions, due to the influence of groundwater, a violation of cationic relations can occur. Precipitation of silica and its modifications from solution during the upwelling of fluids to the surface is also likely. Calculations also show that under natural conditions, the waters are supersaturated with respect to quartz, which leads to a decrease in the concentration of dissolved silicic acid in the discharge zone. The obtained temperatures using the Si-enthalpy mixing model with no steam loss before mixing showed very high temperatures. In the case of the steam separation occurring before the mixing, the obtained reservoir temperatures are close to real ones and differ from the temperatures calculated using Si geothermometers by average 30 °C.

Nevertheless, "classical" geothermometers can fail because the (semi-)empirical correlations on which they are based are not always valid for all geochemical systems. Additionally, geothermal fluids ascending to the ground surface are typically affected by gas loss, mixing and/or dilution with shallower waters, masking their deep geochemical signatures

(Reed and Spycher, 1984). Thus, multicomponent geothermometry presents advantages over classical ones, because it relies on complete fluid analyses and a solid thermodynamic basis, rather than (semi-)empirical correlations and, thus, in principle applies to any geochemical system. The “Fix-Al” method gives more moderate values of temperature for all studied areas except Tavatum (Figure 6). It may be caused by the complexity of the method, which does not take into account that the chemical composition of Tavatum springs may be formed during the dissolution of secondary minerals, formed during the last glaciation, resulting in an overstatement of its reservoir’s temperatures. Calculated temperatures by this method (68–104 °C and 121–153 °C) still reflect two groups of thermal waters confined to two different geological structures. Of course, this method is limited by the proper choice of mineral assemblage the water originates in, usually confirmed by petrology of drilled wells, but we can never be sure about the same minerals, forming the geothermal reservoir itself, as we propose it may be much deeper than the bottom of the well. A trial of calculating the circulation depth, i.e., the depth of geothermal reservoir, may be made using local geothermal gradients. The one for the Okhotsk–Chukotka volcanic belt is 24–28 °C/km, which is slightly higher than for the Sikhote–Alin (24–25 °C/km) [16]. Groundwater circulation depths were estimated for Sikhote–Alin thermal springs spanning an elevation range of 50–300 m.a.s.l. and for the Okhotsk springs spanning an elevation range of 160–691 m.a.s.l. Equilibration temperatures for these springs range from 103 to 136 °C and groundwater circulation depths range from 2.7 ± 0.4 km to 6.1 ± 0.6 km (Table 4). Previously, the depth of the geothermal reservoir within the Sikhote–Alin was estimated at 1–2 km [2,3]. Thus, taking into account the obtained results and the usage limits of the geothermometers, the reservoir temperatures for the Okhotsk Sea Coast thermal waters may be presented as follows in Table 4.

Table 4. Reservoir temperature and circulation depth the studied thermal waters.

Name	$T_{\text{meas.}}, \text{ } ^\circ\text{C}$	$T_{\text{res.}}, \text{ } ^\circ\text{C}$		$T_{\text{res. multicomponent}}, \text{ } ^\circ\text{C}$	Circulation Depth, km
		No Mixing	Mixing		
Tumnin	44	121	159	75	3.0
Annenskie	49	130	162	104	4.1
Ul’skiy	31	103	160	68	2.7
Talaya	70	136	147	121	4.3
Tavatum	59	153		153	6.1

6. Conclusions

The thermal waters of the Sikhote–Alin volcanic belt belong to $\text{HCO}_3\text{--Na}$ type with low TDS (>0.3 g/L) and high pH (>9.1), while waters originating in the Okhotsk–Chukotka volcanic belt belong to $\text{SO}_4\text{--Na}$ and Cl--Ca--Na chemical types, with moderate TDS (1–15 g/L) and alkaline pH (7.5–8.7). All these waters are of meteoric origin feeding from geothermal reservoirs at depths of 2.7–4.1 km and 4.3–6.1 km consequently for the first and the second group.

The article compares several methods for determining the temperature of a deep reservoir for the thermal waters of the Okhotsk Sea coast. In the case of stable low enthalpy geothermal systems, the consequent use of quartz geothermometers gives adequate results. If cold groundwater is mixed into the hydrothermal system in the subsurface horizons, it is necessary to use either different types of cationic geothermometers or mixing models. As long as thermal water is a natural resource of increasing therapeutic importance, geothermometry is still one of the tools for predicting thermal water reservoir temperatures and helping rational resource usage. Nevertheless, the multicomponent method gives more moderate results and may be a useful instrument during commercial use of a natural resource.

Author Contributions: Conceptualization, E.V.Z. and I.V.B.; methodology, E.V.Z. and I.V.B.; software, E.V.Z.; validation, E.V.Z., I.V.B., N.A.K. and G.A.C.; resources, I.V.B., N.A.K. and G.A.C.; writing—original draft preparation, E.V.Z.; visualization, E.V.Z.; supervision, I.V.B.; project administration, I.V.B.; funding acquisition, I.V.B. All authors have read and agreed to the published version of the manuscript.

Funding: The work was carried out with the support of the Russian Science Foundation grant No. 18-77-10007.

Acknowledgments: The authors are grateful to the reviewers for corrections and comments, which hopefully made it possible to significantly improve the manuscript. The work was carried out with the support of the Russian Science Foundation grant No. 18-77-10007.

Conflicts of Interest: The authors declare no conflict of interest.

References

1. Kulakov, V.V.; Sidorenko, S.V. *Mineral Waters and Therapeutic Mud of the Amur Region*; DVGMU: Khabarovsk, Russia, 2017; 473p. (In Russian)
2. Chudaev, O.V. *Composition and Conditions of the Formation of the Modern Hydrothermal Systems of the Russian Far East*; Dal'nauka: Vladivostok, Russia, 2003. (In Russian)
3. Chelnokov, G.; Bragin, I.; Kharitonova, N.; Alexandrov, I.; Ivan, V.; Chelnokova, B. Geochemistry and Conditions of the Formation of the Ulsk Thermal Spring (Coasts of the Sea of Okhotsk, Khabarovsk Krai). *Russ. J. Pac. Geol.* **2019**, *13*, 163–175. [[CrossRef](#)]
4. Chudaev, O.V.; Kharitonova, N.A.; Chelnokov, G.A.; Bragin, I.V.; Kalitina, E.G. *Geochemical Features of the Behavior of Rare-Earth Elements in Waters of the Russian Far East under Conditions of Natural and Anthropogenic Anomalies*; Dal'nauka: Vladivostok, Russia, 2017; 152p. (In Russian)
5. Bragin, I.V.; Chelnokov, G.A.; Chudaev, O.V.; Kharitonova, N.A.; Vysotskiy, S.V. Geochemistry of thermal waters of continental margin of Far East of Russia. *Acta Geol. Sin.* **2016**, *90*, 276–284. [[CrossRef](#)]
6. Bragin, I.V.; Chelnokov, G.A.; Kharitonova, N.A.; Veldemar, A.A.; Pavlov, A.A. Rare-earth elements and isotopic geochemistry of thermal waters of the Okhotsk sea shore, Far East of Russia. *IOP Conf. Ser. Earth Environ. Sci.* **2020**, *467*, 012092. [[CrossRef](#)]
7. Chernyshev, E.I. *Report on Detailed Prospecting of Thermal Waters on the Sea Coast of the Nikolaevsk Region: Works of 1986–1987*; Ul'skii Team: Khabarovsk, Russia, 1988. (In Russian)
8. Bogatkov, N.M.; Kulakov, V.V. Annenskie spa. *Soviet Geol.* **1966**, *5*, 17–19. (In Russian)
9. Polyak, B.G.; Prasolov, E.M.; Lavrushin, V.Y.; Cheshko, A.L.; Kamenskii, I.L. He, Ar, C and N isotopes in thermal springs of the Chukotka Peninsula: Geochemical evidence of the recent rifting in the north-eastern Asia. *Chem. Geol.* **2013**, *339*, 127–140. [[CrossRef](#)]
10. Jeong, C.-H.; Lee, B.-D.; Yang, J.-H.; Nagao, K.; Kim, K.-H.; Ahn, S.-W.; Lee, Y.-C.; Lee, Y.-J.; Jang, H.-W. Geochemical and Isotopic Compositions and Geothermometry of Thermal Waters in the Magumsan Area, South Korea. *Water* **2019**, *11*, 1774. [[CrossRef](#)]
11. Karaku, S.H. Helium and carbon isotope composition of gas discharges in the Simav Geothermal Field, Turkey: Implications for the heat source. *Geochemistry* **2013**, *57*, 213–223. [[CrossRef](#)]
12. Wang, X.; Zhao, L.; Liu, X.; Lili, A.; Zhang, Y. Temperature effect on the transport of nitrate and ammonium ions on a loose-pore geothermal reservoir. *J. Geochim. Exp.* **2013**, *124*, 59–66. [[CrossRef](#)]
13. Lavrushin, V.Y. *Subsurface Fluids of the Greater Caucasus and Its Surrounding*; GEOS: Moscow, Russia, 2012; 349p. (In Russian)
14. Tikhomirov, P.L.; Kalinina, E.A.; Moriguti, T.; Makishima, A.; Kobayashi, K.; Cherepanova, I.Y.; Nakamura, E. The Cretaceous Okhotsk–Chukotka Volcanic Belt (NE Russia): Geology, geochronology, magma output rates, and implications on the genesis of silicic LIPs. *J. Volcanol. Geotherm. Res.* **2012**, *221–222*, 14–32. [[CrossRef](#)]
15. Nokleberg, W.J.; Parfenov, L.M.; Monger, J.W.; Norton, I.O.; Chand'uk, A.I.; Stone, D.B.; Scotese, C.R.; Scholl, D.W.; Fujita, K. Fujita Phanerozoic tectonic evolution of the Circum-North Pacific US Geological Survey. *Prof. Pap.* **2001**, *1626*, 122.
16. Rodnikov, A.G.; Sergeyeva, N.A.; Zabarinskaya, L.P.; Filatova, N.I.; Piip, V.B.; Rashidov, V.A. The deep structure of active continental margins of the Far East (Russia). *Russ. J. Earth. Sci.* **2008**, *10*, ES4002. [[CrossRef](#)]
17. Tolstikhin, O.N. *Hydrogeology of USSR. XXVI. North-Eastern USSR*; Nedra: Moscow, Russia, 1972; 297p. (In Russian)
18. Martynov, A.Y.; Golozubov, V.V.; Martynov, Y.A.; Kasatkin, S.A. Lateral Zonality of the East Sikhote-Alin Volcanic Belt: Geodynamic Regime in the Late Cretaceous. *Russ. J. Pac. Geol.* **2019**, *13*, 265–282. [[CrossRef](#)]
19. Chelnokov, G.; Kharitonova, N.; Bragin, I.; Vasil'eva, M. Deuterium, oxygen-18 and tritium in precipitation, surface and groundwater in the Far East of Russia. *Proc. Earth Planet. Sci.* **2013**, *7*, 151–154. [[CrossRef](#)]
20. Moiseev, A.V.; Luchitskaya, M.V.; Sokolov, S.D. Volcanic Rocks and Granitoids from Cape Svyatoy Nos (Eastern Arctic): Their Age, Composition, and Paleotectonic Reconstructions. *Dokl. Earth Sci.* **2020**, *492*, 2. [[CrossRef](#)]
21. Fournier, R.O. Chemical geothermometers and mixing models for geothermal systems. *Geothermics* **1977**, *5*, 41–50. [[CrossRef](#)]
22. Fournier, R.O. A revised equation for the Na-K geothermometer. *Geotherm. Resour. Counc. Transactions* **1979**, *3*, 221–224.
23. Giggenbach, W.F. Geothermal solute equilibria. Derivation of Na-K-Mg-Ca geothermometers. *Geochim. Cosmochim. Acta* **1988**, *52*, 2749–2765. [[CrossRef](#)]

24. Fournier, R.O.; Truesdell, A.H. An empirical Na-K-Ca chemical geothermometer for natural waters. *Geochim. Cosmochim. Acta* **1973**, *37*, 1255–1275. [[CrossRef](#)]
25. Fournier, R. *Lecture on Geochemical Interpretation of Hydrothermal Waters*; UNU Geothermal Training Programme: Reykjavik, Iceland, 1989; Volume 10, p. 66.
26. Truesdell, A.H.; Fournier, R.O. Procedure for estimating the temperature of a hot water component in mixed water using a plot of dissolved silica vs. enthalpy. *J. Res. USA Geol. Surv.* **1977**, *5*, 49–52.
27. Arnórsson, S.; Gunnlaugsson, E. New gas geothermometers for geothermal exploration calibration and application. *Geochim. Cosmochim. Acta* **1985**, *49*, 1307–1325. [[CrossRef](#)]
28. Fouillac, R.; Michard, S. Sodium/Lithium ratio in water applied to geothermometry of geothermal reservoirs. *Geothermics* **1981**, *10*, 55–70. [[CrossRef](#)]
29. Banks, D.; Sletten, R.S.; Haldorsen, S.; Dale, B.; Heim, M.; Swensen, B. The thermal springs of Bockfjord, Svalbard: Occurrence and major ion hydrochemistry. *Geothermics* **1998**, *27*, 445–467. [[CrossRef](#)]
30. Reed, M.H.; Spycher, N.F. Calculation of pH and mineral equilibria in hydrothermal waters with application to geothermometry and studies of boiling and dilution. *Geochim. Cosmochim. Acta* **1984**, *48*, 1479–1492. [[CrossRef](#)]
31. Pang, Z.-H.; Reed, M.H. Theoretical chemical thermometry on geothermal waters: Problems and methods. *Geochim. Cosmochim. Acta* **1998**, *62*, 1083–1091. [[CrossRef](#)]
32. Palandri, J.; Reed, M.H. Reconstruction of in situ composition of sedimentary formation waters. *Geochim. Cosmochim. Acta* **2001**, *65*, 1741–1767. [[CrossRef](#)]
33. Matsubaya, O.; Sakai, H.; Kusachi, I.; Setake, H. Hydrogen and oxygen isotopic ratios and major element chemistry of Japanese thermal water system. *Geochem. J.* **1973**, *7*, 123–151. [[CrossRef](#)]
34. Frisbee, M.D.; Tolley, D.G.; Wilson, J.L. Field estimates of groundwater circulation depths in two mountainous watersheds in the western U.S. and the effect of deep circulation on solute concentrations in streamflow. *Water Resour. Res.* **2017**, *53*, 2693–2715. [[CrossRef](#)]
35. Kolesar, P.T.; DeGraff, J.V. A comparison of the silica and Na-K-Ca geothermometers for thermal springs in Utah. *Geothermics* **1978**, *6*, 221–226. [[CrossRef](#)]
36. Italiano, F.; Bonfanti, P.; Pizzino, L.; Quattrocchi, F. Geochemistry of fluids discharged over the seismic area of the Southern Apennines (Calabria region, Southern Italy): Implications for fluid-fault relationships. *Appl. Geochem.* **2010**, *25*, 540–554. [[CrossRef](#)]
37. Apollaro, C.; Caracausi, A.; Paternoster, M.; Randazzo, P.; Aiuppa, A.; De Rosa, R.; Fuoco, I.; Mongelli, G.; Muto, F.; Vannia, E.; et al. Fluid geochemistry in a low-enthalpy geothermal field along a sector of southern Apennines chain (Italy). *J. Geochem. Explor.* **2020**, *219*, 106618. [[CrossRef](#)]
38. Shvartsev, S.L.; Sun, Z.; Borzenko, S.V.; Gao, B.; Tokarenko, O.G.; Zippa, E.V. Geochemistry of the thermal waters in Jiangxi Province, China. *Appl. Geochem.* **2018**, *96*, 113–130. [[CrossRef](#)]
39. Shvartsev, S.L.; Zippa, E.V.; Borzenko, S.V. The Nature of Low Salinity and Composition Peculiarities of Thermal Waters in Jiangxi Province (China). *Russ. Geol. Geophys.* **2020**, *61*, 196–213. [[CrossRef](#)]
40. Wang, X.; Wang, G.L.; Gan, H.N.; Liu, Z.; Nan, D.W. Hydrochemical characteristics and evolution of geothermal fluids in the Chabu high-temperature geothermal system, Southern Tibet. *Geofluids* **2018**, *2018*, 8532840. [[CrossRef](#)]
41. Lin, S.-S.; Shen, S.-L.; Zhou, A.; Lyu, H.-M. Assessment and management of lake eutrophication: A case study in Lake Erhai, China. *Sci. Total Environ.* **2021**, *751*, 141618. [[CrossRef](#)]
42. Lyu, H.-M.; Shen, S.-L.; Zhou, A. The development of IFN-SPA: A new risk assessment method of urban water quality and its application in Shanghai. *J. Clean. Prod.* **2021**, *282*, 124542. [[CrossRef](#)]
43. Lyu, H.-M.; Shen, S.-L.; Wu, Y.-X.; Zhou, A.-N. Calculation of groundwater head distribution with a close barrier during excavation dewatering in confined aquifer. *Geosci. Front.* **2021**, *12*, 791–803. [[CrossRef](#)]
44. Alçiçek, H.; Bülbül, A.; Brogi, A.; Liotta, D.; Ruggieri, G.; Capezzuoli, E.; Meccheri, M.; Yavuzer, I.; Alçiçek, M.C. Origin, evolution and geothermometry of the thermal waters in the Gölemezli Geothermal Field, Denizli Basin (SW Anatolia, Turkey). *J. Volcanol. Geotherm. Res.* **2018**, *349*, 1–30. [[CrossRef](#)]
45. Keenan, J.H.; Keyes, F.G.; Hill, P.G.; Moore, J.G. *Steam Tables—Thermodynamic Properties of Water including Vapor, Liquid, and Solid Phases*, International Edition—Metric units ed.; Wiley: New York, NY, USA, 1969; p. 162.
46. Chudaev, O.V.; Chelnokov, G.A.; Bragin, I.V.; Kharitonova, N.A.; Rychagov, S.N.; Nuzhdaev, A.A.; Nuzhdaev, I.A. Geochemical features of major and rare-earth element behavior in the Paratunka and Bol’shebanni hydrothermal systems of Kamchatka. *Russ. J. Pac. Geol.* **2016**, *10*, 458–475. [[CrossRef](#)]
47. Chelnokov, G.A.; Kharitonova, N.A.; Bragin, I.V.; Aseeva, A.V.; Bushkareva, K.Y.; Liamina, L.A. The Geochemistry of Rare Earth Elements in Natural Waters and Secondary Mineral Sediments of Thermal Fields of Kamchatka. *Mosc. Univ. Geol. Bull.* **2020**, *75*, 196–204. [[CrossRef](#)]